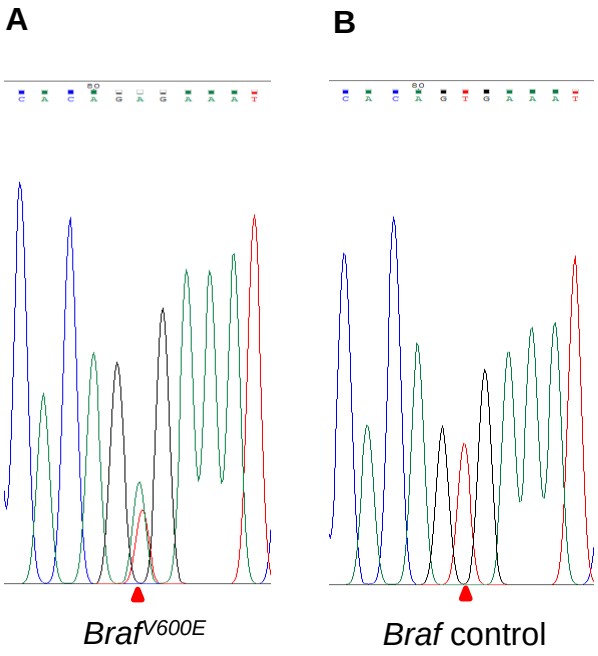

Supplementary Figure 1-Presence of *Braf*^{V600E} mutation in organoids verified by Sanger sequencing. gDNA prepared from 4-hydroxy tamoxifen treated organoids from *Villin*^{CreERT}*; Braf*^{CA} mice (*A*) or vehicle treated controls (B).

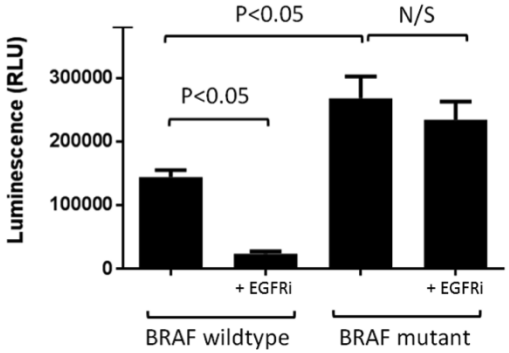

Supplementary Figure 2-Functional Braf^{V600E} in colonic organoids results in increased cellular proliferation and resistance to epidermal growth factor receptor inhibitor (EGFRi) treatment. Quantification of metabolically active cells using Real Time-Glo in *Braf* wild-type or *Braf*^{V600E} mutant mouse colonic organoid cultures after treatment with vehicle or EGFRi. Control cells did not survive in the presence of EGFRi, whilst *Braf*^{V600E} organoids were resistant. Representative experiment conducted in triplicate, error bars denote st.dev.

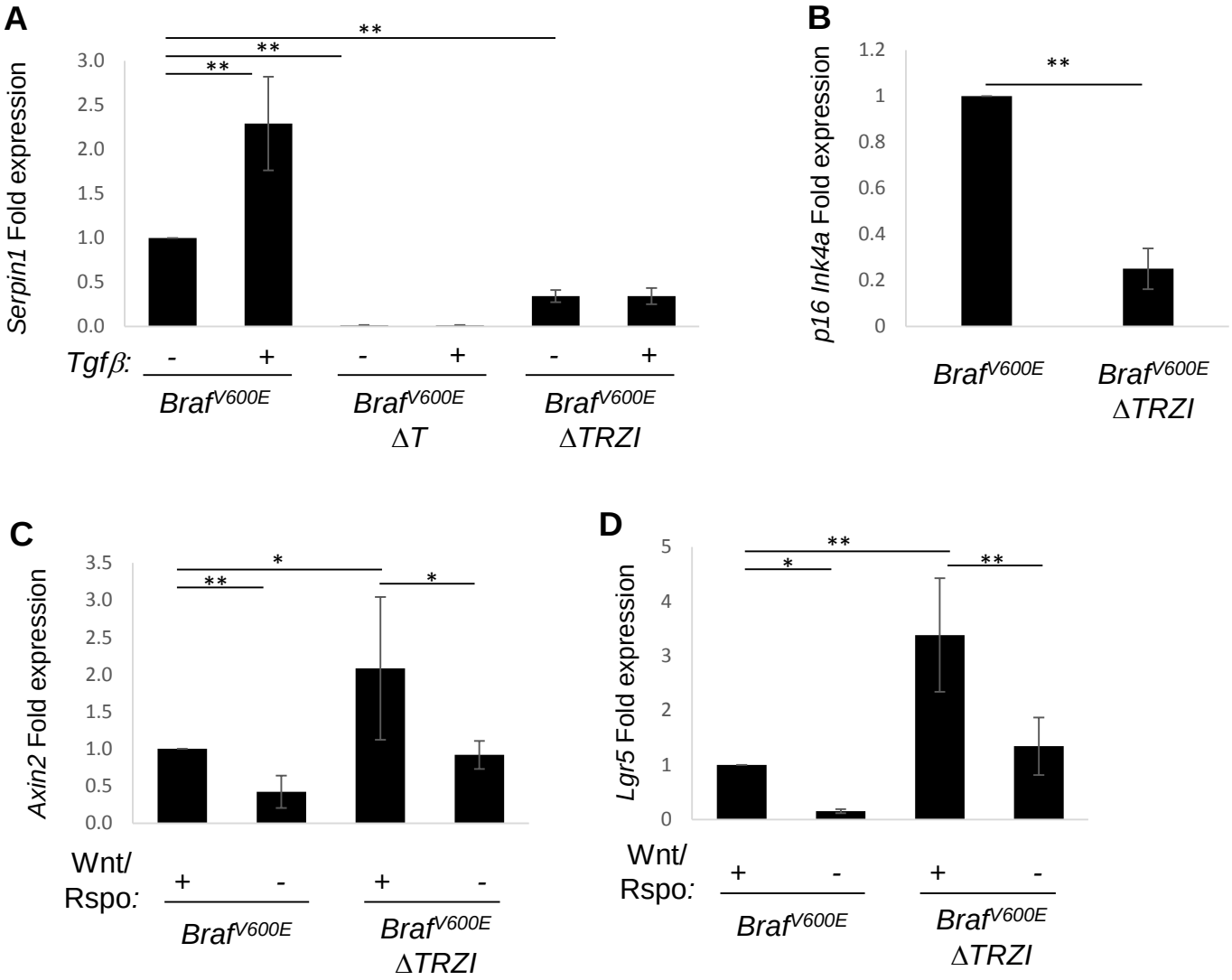

Supplementary Figure 3. **A,** Expression of *Serpin-1*, a Tgfβ response gene, is not induced following treatment with Tgfβ in *Tgfβr2* mutant organoids. **B,** *p16Ink4a* RNA levels are decreased in *p16Ink4a* mutant organoids. **C-D,** Transcript levels of two Wnt-responsive genes, *Axin2* and *Lgr5*, are increased in organoids with mutations in the two negative regulators of the Wnt-pathway, *Rnf43* and *Znrf3*. Fold induction of mRNA expression is normalized to *Gapdh*, with transcript level in *Braf*^{V600E} organoids in complete medium set to 1. Results from at least three independent experiments performed in triplicate are shown, error bars denote standard deviation. Two-tailed t-test was used for pair-wise statistical analysis. *=p≤0.05, **=p≤0.01.

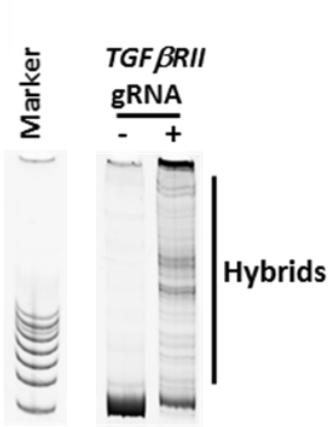

Supplementary Figure 4. Effective targeting of genes associated with serrated CRC using CRISPR/Cas9 gene editing followed by media selection of correctly targeted clones. **A,** Melt/reanneal of PCR amplicons from *Tgfβr2* targeted genomic region in edited clones show the formation of hybrid complexes (slower migrating bands) in the presence of specific gRNAs but not the empty gRNA control by PAGE.

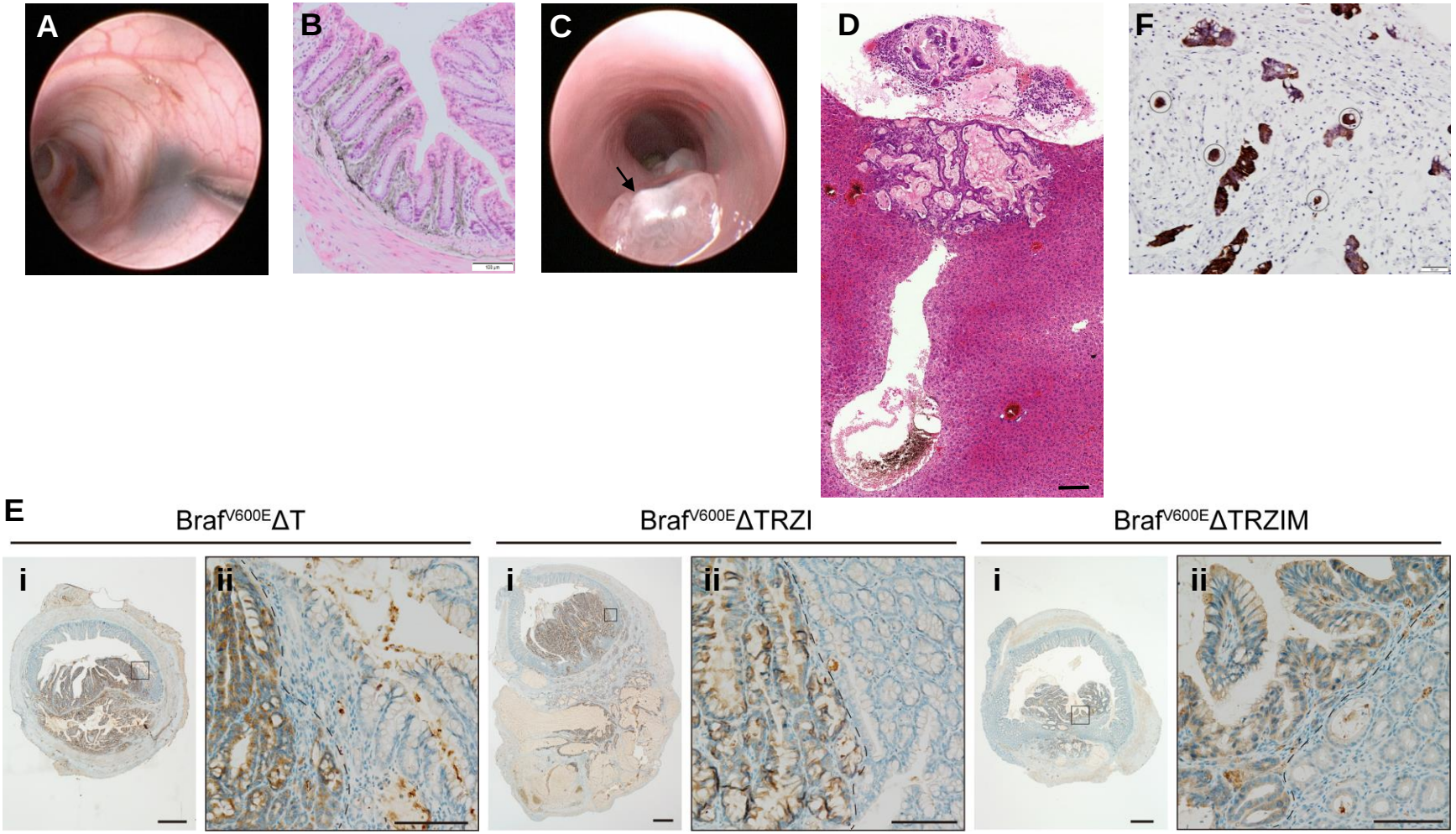

Supplementary Figure 5. Orthotopic injection site in colon wall. **A**, Colonoscopic image with needle and dark ink spots at injection sites and **B**, histological location of injected dye immediately adjacent to the colonic epithelium in the mucosal layer. **C,** Representative colonoscopy image of *Braf^{V600E}ΔTRZI* tumours showing white mucous cap on *Braf^{V600E}ΔTRZI* tumours (arrow). **D,** histology of infrequent liver metastasis (n=1 from 11 mice) in *Braf^{V600E}ΔTRZI* injected animals. **E,** low (i) and high (ii) power images of immunohistochemical staining for mutant BrafV600E protein in serratoid derived tumour cells. These are the same samples as depicted in Figure 4D but here high power image focusses on part of the section with tumour (to left of dashed line in ii) and normal epithelium (to right of dashed line in ii). **F,** tumour budding (circled) from *Braf^{V600E}ΔTRZI* tumours is positive for cytokeratin 20 (CK20) by immunohistochemistry. Scale bars 500um (Ei), 100um (B, D Eii), 50um (F).

A

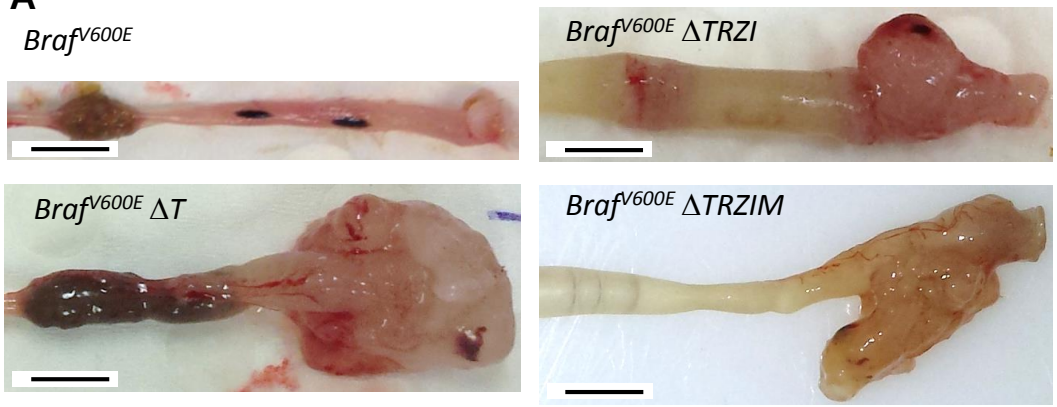

B

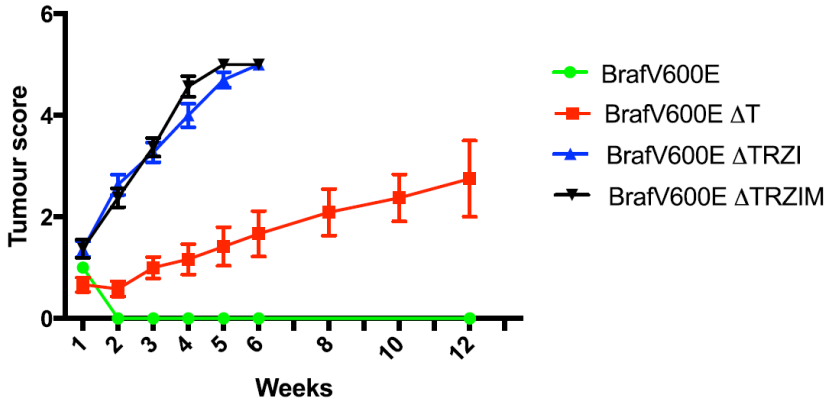

Supplementary Figure 6. A, Necropsy images of dissected distal colon showing ink spots only following *Braf*^{V600E} organoid injections and invasion/extra-colonic growth from more complex organoid lines. Scale bar is 0.5cm. **B,** Colonoscopic scoring of largest tumour in each mouse (n=5 mice per group, Becker scale). Extended time course for tumour scoring to show relatively slow growth of *Braf*^{V600E} *ΔT* tumours out to 12 weeks (Figure 3C depicts the same data but finishes at 6weeks).

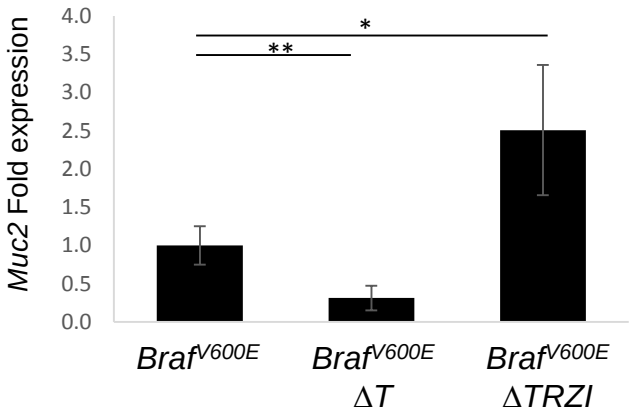

Supplementary Figure 7. Expression *Muc2*, a goblet cell marker and core component of the mucus layer is increased in *Braf*^{V600E}*ΔTRZI* but not *Braf*^{V600E}*ΔT* mutant organoids. Fold induction of mRNA expression is normalized to *Gapdh*, with transcript level in *Braf*^{V600E} organoids in complete medium set to 1. Results from at least three independent experiments performed in triplicate are shown, error bars denote standard deviation. Two-tailed t-test was used for pair-wise statistical analysis. *=p≤0.05, **=p≤0.01.

A

	Microsatellite Markers				
	mBat-26	mBat-67	mBat-37	GA29	TG27
Organoid donor mouse gDNA	wt	wt	wt	wt	wt
BrafV ΔTRZI Organoids	wt	wt	wt	wt	wt
Colon tumours generated by orthotopic injection of *BrafV ΔTRZI* Organoid (n=5)	wt	wt	wt	wt	wt
	wt	wt	wt	wt	wt
	wt	wt	wt	wt	wt
	wt	wt	wt	wt	wt
	wt	wt	wt	wt	wt
BrafV ΔTRZIM Organoid Line 1 (*Mlh1*$^{\Delta/\Delta}$)	1bp Del	3bp Del	1bp Del	wt	wt
BrafV ΔTRZIM Organoid Line 2 (*Mlh1*$^{\Delta/\Delta}$)	ND	ND	1bp Del	wt	2bp Del
BrafV ΔTRZIM Organoid Line 3 (*Mlh1*$^{\Delta/+}$)	ND	ND	1bp Del	wt	wt
Colon tumours generated by orthotopic injection of *BrafV ΔTRZIM* Organoid Line 1 (n=6)	2bp Del	5bp Del + 32bp Del	3bp Del	wt	wt
	1bp Del	4bp Del	wt	wt	wt
	1bp Del	5bp Del	1bp Ins	wt	wt
	1bp Del	4bp Del + 22bp Del	1bp Del	wt	wt
	1bp Del	4bp Del + 22bp Del	1bp Del	wt	wt
	1bp Del	4bp Del + 22bp Del	wt	wt	wt

B

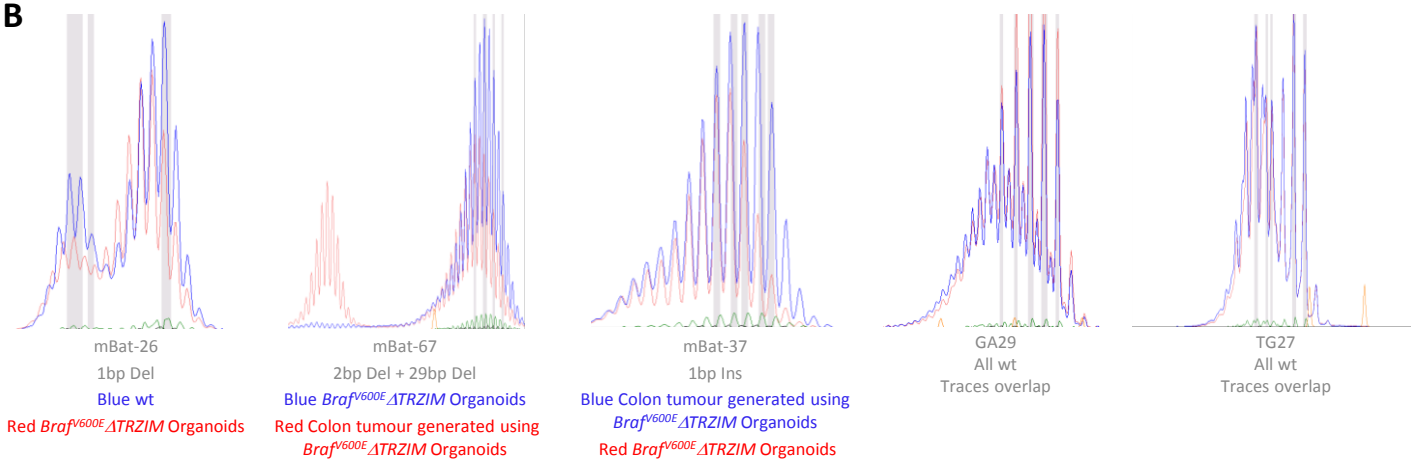

Supplementary Figure 8. Analysis of microsatellite instability using 5 validated mouse microsatellite markers. **A,** repeat tract length for 5 validated mouse microsatellite markers shows variability (MSI) in *Mlh* mutant organoids and tumours, ND not determined. **B,** representative sequence traces of microsatellite marker length.

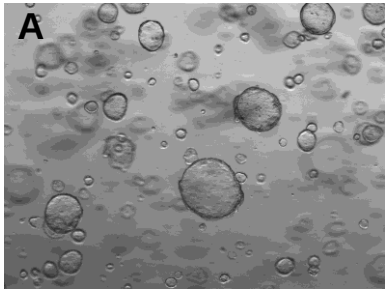

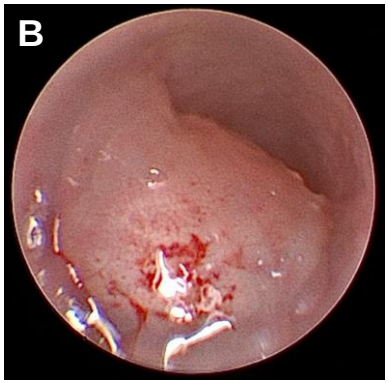

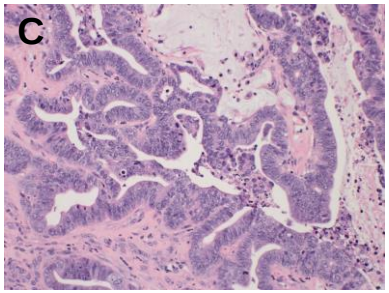

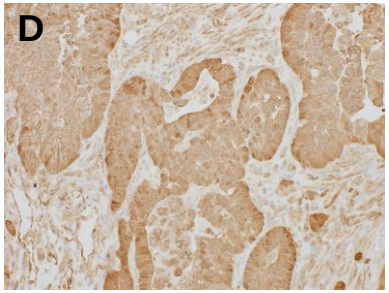

Supplementary Figure 9. A, colonic organoids derived from *Kras*$^{LSL\text{-}G12D/+}$;*Apc*$^{fl/fl}$ mice, that were treated with Ad5CMV::Cre survived culture in the absence of Wnt3a or Rspo1. **B,** colonoscopic image showing orthotopic growth of *Kras*$^{G12D/+}$;*Apc* $^{\Delta 580l/\Delta 580}$ organoids. **C,** H&E and **D,** Ctnnb1 immunohistochemistry of *Kras*$^{G12D/+}$;*Apc* $^{\Delta 580l/\Delta 580}$ tumours (20x). Genotyping of transgenic alleles confirm **(E)** homozygous recombination of the floxed *Apc* locus and **(F)** heterozygous recombination of the floxed *Kras* locus.

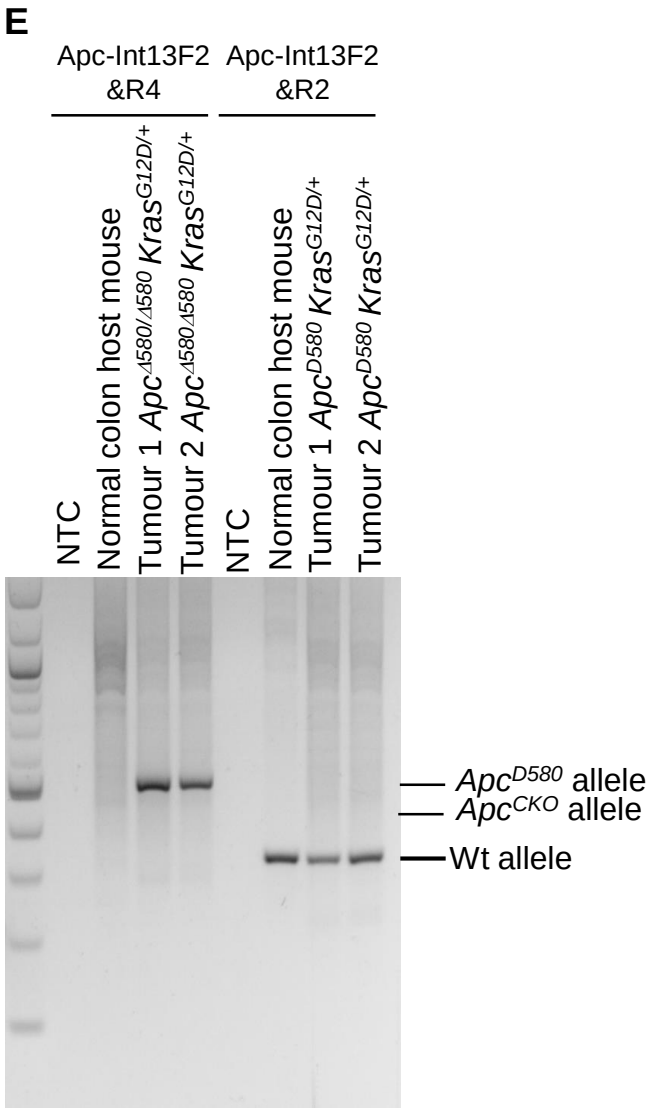

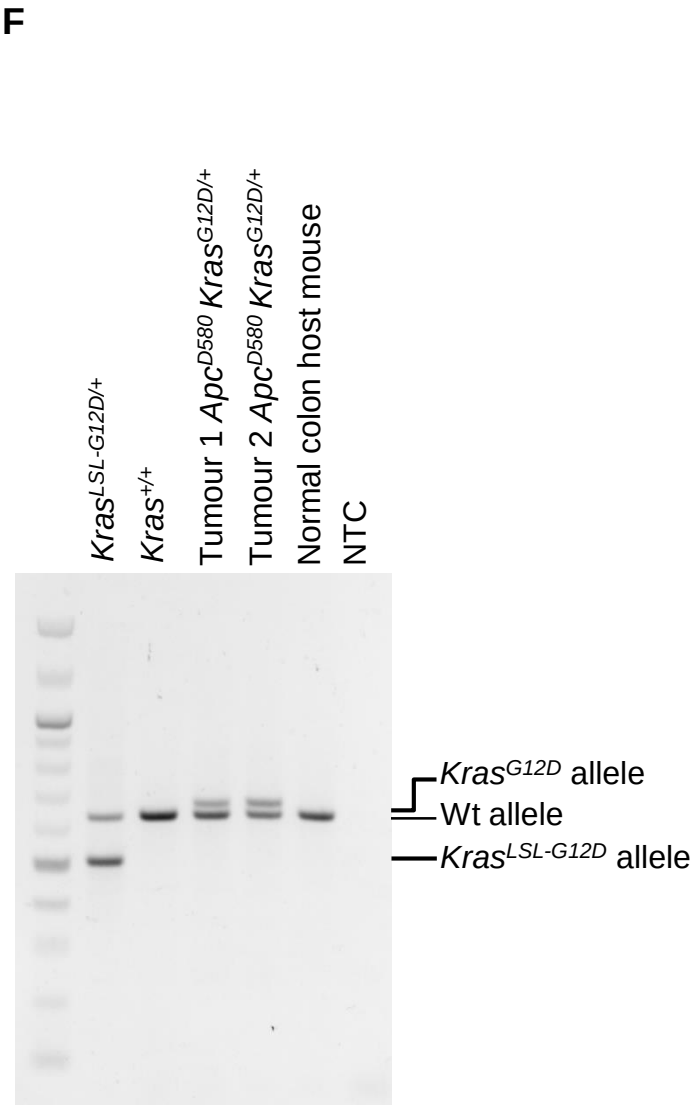

Supplementary Table 1-Sanger sequencing the top bioinformatically predicted *Tgfbr2* and *Bmpr2* gRNA off-target sites reveals no off-target events in mutant organoid lines.

	Location	Sequence	Mismatches	Strand	Type	Comments-sequencing each locus in gDNA isolated from CRISPR/Cas9 gene edited organoid
Tgfbr2 gRNA On-site	9:116174992-116175014	GGACGATATGCAGCGGCCAC AGG	0	+	Exonic	
Tgfbr2_off_site1	18:65431501-65431523	GGAAGATATGAAGGGGCCAC TGG	3	-	Intronic	No change compared to reference mouse genome
Tgfbr2_off_site2	13:74221583-74221605	**GGACCATATGCAGTGGTCAC AGG**	3	+	Intronic	No change compared to reference mouse genome
Tgfbr2_off_site3	12:26345670-26345692	GGCTCACATGCAGCGGCCAC AGG	4	-	Intronic	No change compared to reference mouse genome
Tgfbr2_off_site4	4:74305539-74305561	GGAGCTTATGCAGAGGCCAC AGG	4	-	Intronic	Repeat sequence, Sanger sequencing not possible
Tgfbr2_off_site5	4:124246525-124246547	**GGAAGAGAAGCAGAGGCCAC AGG**	4	+	Intergenic	No change compared to reference mouse genome
Tgfbr2_off_site6	1:87663023-87663045	**GGACGGGAAGCAGAGGCCAC TGG**	4	+	Intronic	No change compared to reference mouse genome
Tgfbr2_off_site7	7:69437642-69437664	GGACCATGTGAAGGGGCCAC TGG	4	-	Intergenic	No change compared to reference mouse genome
Tgfbr2_off_site8	12:118438479-118438501	**GGATTATATGCACAGGCCAC TGG**	4	+	Intergenic	No change compared to reference mouse genome
Tgfbr2_off_site9	8:13155901-13155923	**GGAATATATGCAAAGGCCAC AGG**	4	+	Intergenic	No change compared to reference mouse genome
Tgfbr2_off_site10	6:29249997-29250019	GGAAGATATGAAAAGGCCAC AGG	4	-	Intergenic	No change compared to reference mouse genome

	Location	Sequence	Mismatches	Strand	Type	Comments-sequencing each locus in gDNA isolated from CRISPR/Cas9 gene edited organoid
Mlh1 gRNA On-site	9:111271459-111271481	TAGTGAACCGCATAGCGGCG GGG	0	-	Exonic	
Mlh1_Off_Site1	12:99158597-99158619	CAGTGAACAGCATAGCGGGG AGG	3	-	Intergenic	No change compared to reference mouse genome
Mlh1_Off_Site2	14:53741961-53741983	TAGTAAACAGCAGCGCGGCG AGG	4	+	Intergenic	Identical to reference mouse genome except for SNP:rs579384457. This SNP present in parental mouse gDNA, i.e. not an off-target event.
Mlh1_Off_Site3	15:84631904-84631926	TAGAGAACAGCATGGGGCG GGG	4	-	Intergenic	No change compared to reference mouse genome
Mlh1_Off_Site4	15:36853646-36853668	**TAGTGATCCCCATAGGGCCG GGG**	4	+	Intergenic	No change compared to reference mouse genome
Mlh1_Off_Site5	9:69989986-69990008	**TAGTGCACCCCATAGCCTCG GGG**	4	+	Intronic	No change compared to reference mouse genome
Mlh1_Off_Site6	10:61247708-61247730	**TAGAGAAACGCAGAGCGGGG AGG**	4	+	Intronic	No change compared to reference mouse genome
Mlh1_Off_Site7	5:137788331-137788353	**TACTGAACCCCACAGCGGAG GGG**	4	-	Intronic	No change compared to reference mouse genome
Mlh1_Off_Site8	8:50161834-50161856	TAGTGAACAACAGAGCGGGG GGG	4	-	Intergenic	Repeat sequence, Sanger sequencing not possible
Mlh1_Off_Site9	1:143952103-143952125	TAGAGAACCACATAGTGGTG TGG	4	-	Intergenic	No change compared to reference mouse genome

Supplementary Table 2. Loss of function insertions/deletions (indels) at target sites using CRISPR/Cas9 combined with media selection for correctly targeted organoid clones. Sanger sequencing of each target site allele and resulting change to protein sequence is displayed in the table below. N.B.* we sequenced 7 plasmid clones containing PCR-amplified *p16Ink4a* target genomic sequence and all were identical. This suggests that likely both alleles were altered in an identical manner or a larger deletion has removed the PCR primer sites at the target site for allele 2.

	wt protein	**DNA Δ**	**Change to Protein**	**DNA Δ**	**Change to Protein**
		Allele 1		**Allele 2**	
Rnf43	784 aa	5bp del	p.R246fs* (premature stop 250aa)	10bp del	p.R246fs* (premature stop 272aa)
Znrf3	913 aa	3bp del	p.T308*del* (912aa)	4bp ins	p.T308*ins** (premature stop 337aa)
Tgfβr2	567 aa	13bp del	p.L9fs* (premature stop 51aa)	339bp del	Removes +1ATG translation start site
p16Ink4a	168 aa	1 bp del	p. S34fs* (premature stop 42aa)	*	
Mlh1	760 aa	31bp del	p.L10fs* (premature stop 24aa)	*2bp ins+12bp del*	p.A19fs* (premature stop 31aa)

	Tumour ID	Type	Serrated Features										Desmoplastic stromal reaction	Infiltrative growth	Tumour budding
			eosinophilic cytoplasm	abundant cytoplasm	basal nuclei	vesicular nuclei	prominent nucleolus	luminal serrations	absence of necrosis	mucin	cell balls and papillary rods	Total score			
Braf^{V600E} *ΔT* (n=6)	402	Adenocarcinoma	1	0	0	1	1	0	1	0	0	4	Minimal	Present	Absent
	197	Adenocarcinoma	0	0	1	1	0	0	1	0	0	3	Present	Present	Absent
	199	Adenocarcinoma	0	0	1	0	0	1	1	0	0	3	Minimal	Present	Absent
	457	Adenocarcinoma	0	0	1	1	1	0	1	0	0	4	Minimal	Present	Absent
	401	Adenocarcinoma	1	0	1	1	1	0	1	1	1	7	Present	Present	Absent
	403	Adenocarcinoma	0	0	0	0	0	0	1	0	0	1	Absent	Present	Absent
Braf^{V600E} *ΔTRZI* (n=14)	348	High grade tubulovillous adenoma	0	0	0	0	0	0	1	0	0	1	Absent	Absent	Absent
	349	Adenocarcinoma	0	0	0	1	1	0	1	1	0	4	Present	Absent	Absent
	351	Mucinous adenocarcinoma	0	0	0	0	0	0	1	1	1	3	Present	Present	Present (low level)
	352	Adenocarcinoma	0	0	0	1	1	0	1	0	0	3	Absent	Present	Absent
	353	Mucinous adenocarcinoma	0	0	0	0	0	0	1	1	1	3	Present	Present	Present (low level)
	354	Mucinous adenocarcinoma	0	0	0	0	0	0	1	1	1	3	Present	Present	Absent
	112	Mucinous adenocarcinoma	0	0	1	0	0	0	1	1	0	3	Present	Present	Present (low level)
	111	Adenocarcinoma	0	0	1	1	0	0	1	1	0	4	Present	Present	Absent
	109	Adenocarcinoma	0	0	1	0	0	0	1	1	1	4	Present	Present	Absent
	108	Adenocarcinoma	0	0	1	0	0	0	1	1	0	3	Present	Present	Absent
	107	Adenocarcinoma	0	0	1	1	0	0	1	1	0	4	Present	Present	Present (low level)
	106	Adenocarcinoma	0	0	1	0	0	0	1	1	0	3	Present	Present	Present (low level)
	105	Mucinous adenocarcinoma	0	0	0	0	0	0	1	1	1	3	Present	Present	Present (low level)
Braf^{V600E} *ΔTRZIM* (n=6)	516	Adenocarcinoma	0	0	0	0	0	0	1	0	0	1	Absent	Absent	Absent
	517	Mucinous adenocarcinoma	0	0	0	0	0	0	1	1	1	3	Present	Present	Absent
	518	Adenocarcinoma	0	0	0	0	0	0	0	0	0	0	Absent	Present	Absent
	519	Mucinous adenocarcinoma	0	0	0	0	0	0	1	1	1	3	Present	Present	Absent
	566	Mucinous adenocarcinoma	0	0	0	0	0	0	1	1	1	3	Present	Present	Present (low level)
	567	Adenocarcinoma	0	0	0	1	1	0	1	0	0	3	Minimal	Absent	Absent

Supplementary Table 3. Pathology scoring of mouse tumours for type (WHO classification 4th Ed, 2010), serrated features common to human serrated adenocarcinoma (WHO classification 4th Ed, 2010), the desmoplastic stromal reaction, infiltrative growth and tumour budding properties.

	ES	NES	NOM.p val	FDR q-val
Top 5 GSEAs *Braf^{V600E} ΔT* tumour vs normal colon				
REACTOME_SPHINGOLIPID_DE_NOVO_BIOSYNTHESIS	0.539	2.629	0.00	0.013
REACTOME_SPHINGOLIPID_METABOLISM	0.494	2.276	0.00	0.013
KEGG_LYSOSOME	0.452	2.147	0.00	0.018
KEGG_TOLL_LIKE_RECEPTOR_SIGNALING_PATHWAY	0.581	1.989	0.00	0.015
KEGG_CHEMOKINE_SIGNALING_PATHWAY	0.638	1.948	0.00	0.016
Top 5 GSEAs *Braf^{V600E} ΔTRZI* tumour vs normal colon				
REACTOME_SPHINGOLIPID_DE_NOVO_BIOSYNTHESIS	0.45	2.267	0.00	0.028
KEGG_LEISHMANIA_INFECTION	0.743	2.145	0.00	0.023
KEGG_TOLL_LIKE_RECEPTOR_SIGNALING_PATHWAY	0.556	2.061	0.00	0.022
ST_ERK1_ERK2_MAPK_PATHWAY	0.578	2.045	0.00	0.023
REACTOME_DEADENYLATION_OF_MRNA	0.523	1.97	0.00	0.031
Top 5 GSEAs *Braf^{V600E} ΔTRZIM* tumour vs normal colon				
REACTOME_SPHINGOLIPID_DE_NOVO_BIOSYNTHESIS	0.502	2.526	0.00	0.013
KEGG_APOPTOSIS	0.389	2.027	0.00	0.038
ST_P38_MAPK_PATHWAY	0.39	1.93	0.00	0.030
KEGG_LEISHMANIA_INFECTION	0.672	1.889	0.00	0.027
KEGG_RIG_I_LIKE_RECEPTOR_SIGNALING_PATHWAY	0.348	1.88	0.00	0.030
Top 5 GSEAs in *Kras^{G12D}Apc$^{Δ/Δ}$* tumour vs normal				
REACTOME_EGFR_DOWNREGULATION	0.439	2.058	0.00	0.055
REACTOME_ANTIVIRAL_MECHANISM_BY_IFN_STIMULATED_GENES	0.33	1.662	0.00	1.000
KEGG_CITRATE_CYCLE_TCA_CYCLE	0.607	1.621	0.00	0.723
KEGG_PYRUVATE_METABOLISM	0.597	1.619	0.00	0.683
REACTOME_GLUCONEOGENESIS	0.595	1.604	0.00	0.644

Supplementary Table 4. Top 5 gene sets enriched for each pair-wise comparison of normal mouse colon with tumour samples. Nominal p values (NOM.p val) all <0.001. Enrichment score (ES), false discovery rate (FDR), normalized enrichment score (NES).

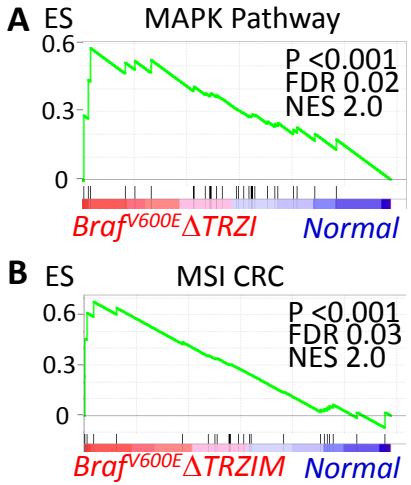

Supplementary Figure 10. GSEA identified differential expression of **(A)** ERK1/2 MAPK pathway transcripts in the *Braf*^{V600E}*ΔTRZI* tumours and **(B)** transcripts up-regulated in a human MSI-CRC gene set (Watanabe *et al*., Cancer Res 2006;66:9804-8) in the *Braf*^{V600E}*ΔTRZIM* tumours compared to normal colon. Enrichment score (ES), false discovery rate (FDR), normalized enrichment score (NES).

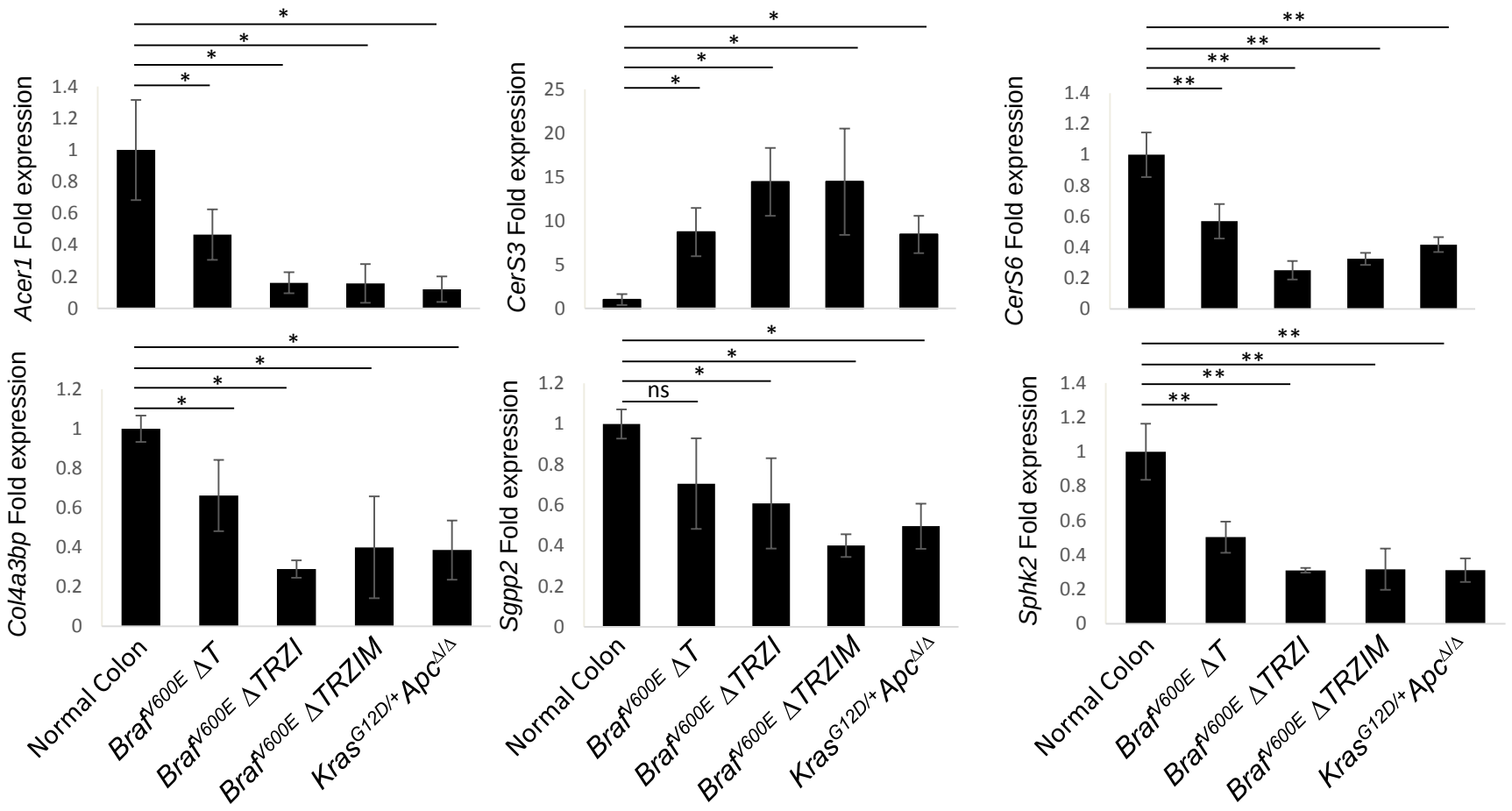

Supplementary Figure 11. Differential expression of spingolipid metabolism transcripts in normal mouse colon and tumours generated from *Braf*^{V600E} organoid series and *Kras*$^{G12D/+}$*Apc*$^{\Delta/\Delta}$organoids. qPCR validation of RNAseq leading edge genes from GSEA. Expression of *CerS3* is increased and *Acer1, CerS6, Col4a3bp, Sgpp2, Sphk2 are* decreased in tumours compared to normal colon. Fold induction of mRNA expression is normalized to *Gapdh*, with transcript level in normal colon set to 1. Results from at least four animals with triplicate technical replicates are shown, error bars denote standard deviation. Two-tailed t-test was used for pair-wise statistical analysis. ns=not significant, *=p≤0.05, **=p≤0.01.